

Beyond α -Helix and β -Sheet: the Expanding Role of Circular Dichroism

Perceived for many years as a low-resolution biophysical technique, CD spectroscopy has advanced well beyond its conventional textbook description. This white paper highlights the expanding role of CD as it undergoes a fundamental transition from its origins in basic academic research to becoming an indispensable tool for the biopharmaceutical industry—a biophysical characterization technique that offers far more than the proportion of α -helix and β -sheet in a protein.

- Near-UV CD spectra reveal minor changes in tertiary structure, complementing the traditional use of far-UV scans to detect change in secondary structure
- Objective, statistically-validated higher order structure (HOS) comparisons of CD spectra confirm similarities or differences between samples, replacing subjective, visual comparisons
- Comprehensive information about structure and stability is revealed in a single continuous, multi-wavelength thermal denaturation experiment

In short, state-of-the-art CD analysis provides unique insights into changes in secondary and tertiary structure, as well as kinetic and thermodynamic information, enabling researchers to publish with confidence and contributing to informed decision-making during biotherapeutic development.

Section 1

The Changing Role of CD Analysis

A brief overview of how CD has moved beyond α -helix and β -sheet to become a critical tool for biomolecular characterization.

Section 2

Protein Secondary and Tertiary Structure in Focus

Using NISTmAb, a monoclonal antibody reference material, we show how modern CD spectrometers provide detailed insight into the secondary and tertiary structure of proteins. Offered by the National Institute of Standards and Technology, U.S. Department of Commerce, the NISTmAb standard enables scientists to evaluate the performance of methods used to determine physicochemical and biophysical attributes of monoclonal antibodies.

Section 3

Assessing Protein Stability Through Thermal Denaturation

Including an introduction to the theory and practice of thermal denaturation experiments, this section features a case study demonstrating characterization of the thermal stability of a biomolecule using CD and fluorescence measurements.

Section 4

Evaluating Statistical Significance of Changes Detected in Higher Order Structure

As the biopharmaceutical industry faces increasing demands for objective, statistically-validated data in regulatory submissions, state-of-the-art CD spectrometry enables detection of minor changes in higher order structure (HOS) and evaluation of their statistical significance - exemplified in this section by a forced degradation study of a monoclonal antibody.

Section 5

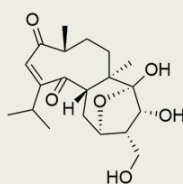
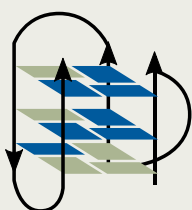
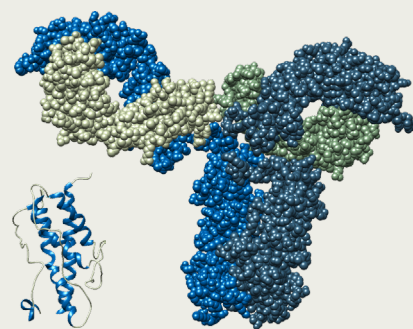
The Physical Principles Behind Circular Dichroism

For those new to CD spectroscopy, or as a refresher for experienced users, this section covers the basic physical principles behind the technique

1. The Changing Role of CD Analysis

Today, circular dichroism (CD) spectroscopy is used throughout academic research and in the biopharmaceutical industry to provide insight into the structure and stability of any molecule containing **chiral elements** (Box 1).

Box 1: Typical applications of CD Spectroscopy



- Higher Order Structure (HOS) comparisons during biotherapeutic development
- Influence of stress or storage conditions on biotherapeutics
- Conformation and stability of proteins and nucleic acids
- Biomolecule-biomolecule interactions, involving proteins, peptides, nucleic acids and small ligands
- Interaction of biomolecules with nanomaterials, e.g. nanoparticles as drug delivery systems
- Characterization of newly synthesized compounds or isolates from natural sources
- Determination of binding constants or rate constants
- Thermodynamics of unfolding/refolding
- Stereo-specificity in biochemical pathways

Functional Materials
Biotherapeutics
Food Compounds
Nanobiologics
Small Molecules
Proteins
Polymers
Antibodies
Aptamers
DNA
Peptides
G-Quadruplexes
Amyloid Fibrils
RNA
Hydrogels
Organometallic Complexes

Thanks to technological advances in CD spectroscopy, applications now go far beyond the assessment of α -helix and β -sheet content of proteins. Most scientists use state-of-the-art Chirascan™ CD spectrometers to monitor changes in secondary and tertiary structure and to investigate the stability of proteins and peptides. Others use CD in nucleic acids research, for example, to study G quadruplexes, intercalating ligands or RNA-protein

interactions ([1]-[3]). The technique is also frequently used to characterize synthetic small molecules or natural compounds with pharmaceutical potential and to study organometallic complexes. More recently, CD spectroscopy has been gaining importance in emerging scientific fields including the study of nanomaterials such as nanoparticles, and functional macromolecules including non-biological polymers such as hydrogels ([4]).

However, it is in biomolecular characterization where the contribution of CD is expanding most rapidly, driven by a need to understand disease mechanisms, identify new drug targets, develop new biotherapeutics and vaccines, and new drug delivery systems.

2. Protein Secondary and Tertiary Structure in Focus

CD spectroscopy is an orthogonal technique within the biophysical characterization toolbox used in academia and the biopharmaceutical industry to study biomolecules, in particular, proteins and peptides. Compared to other methods for similar applications, its versatility is unique, yielding information about both secondary and tertiary structure, as well as the stability of a protein, with minimal requirements for sample preparation.

The **secondary structure** of a protein refers to the local structural elements stabilized predominantly by short-range interactions within the protein backbone—mainly hydrogen bonds formed between amino acids that are often in close vicinity within the protein sequence (the **primary structure**). The most common of such elements are α -helices, as found in insulin, and β -strands that typically make up larger β -sheets, the dominant elements in monoclonal antibodies. However, other secondary structure elements are known to exist. For example, there are different types of helices and turns, and β -sheets can be pleated or twisted. Several of these sub-elements can be found even within a rather small protein.

The **tertiary structure** of a protein is its overall three-dimensional arrangement, stabilized by long-range interactions such as electrostatic and hydrophobic interactions, salt bridges and disulfide bonds. These interactions are formed between the side chains of amino acids that can be far apart from each other in the sequence yet are close together spatially.

The **principle chromophores** in proteins that interact with **circularly polarized light** as used in CD spectroscopy (Section 5) are the peptide bonds, aromatic amino acids and disulfide bonds (Figure 1). The α -carbon

atoms of amino acids are the chiral centers in the protein backbone, and the absorbance of circularly polarized light by **peptide bonds** gives rise to typical CD signals at low wavelengths between 180 and 250 nm. This wavelength range is the so-called **far-UV** (as it is distant from the visible range of the electromagnetic spectrum) containing information about the secondary structure. The side chains of the **aromatic amino acids** are chromophores that give rise to CD signals despite being non-chiral because they are affected by the chiral environment in which they reside. Corresponding CD signals are obtained in a range at higher wavelengths between 250 and 350 nm, the **near-UV** (closer to the visible spectral range), containing information about the tertiary structure. Disulfide bonds can contribute to both the far- and near-UV.

Spectral bands in the far-UV are characteristic for secondary structure elements that adopt a similar arrangement in different proteins: for example, a high content of α -helices gives rise to a positive peak at about 190 nm and two negative peaks at about 208 and 222 nm. In contrast, a near-UV CD spectrum can be considered more as a **fingerprint** region because its profile very much depends on the type and number of aromatic amino acids and their environment and thus dif-

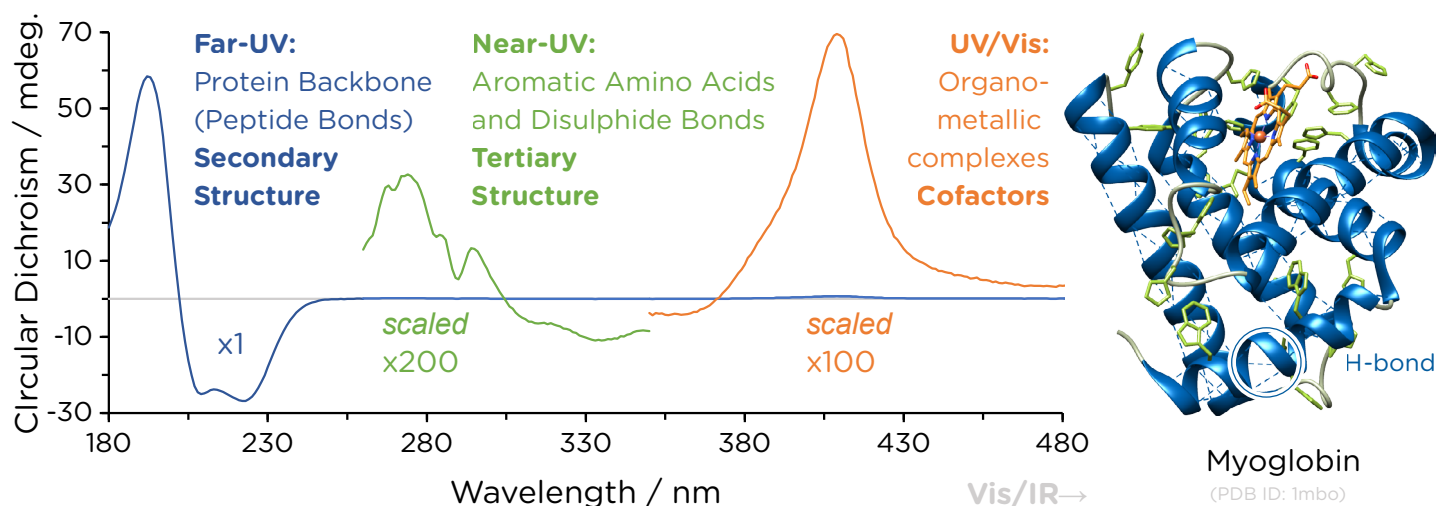
fers substantially between individual proteins.

Obtaining information about both secondary and tertiary structure by CD usually requires **two separate measurements**. This is because aromatic amino acids are less abundant in a protein than peptide bonds, so a much higher protein concentration (under otherwise identical experimental conditions) is required to obtain an adequate signal in the near-UV as compared with the far-UV.

For proteins such as myoglobin that contain prosthetic groups which absorb in the visible range of the electromagnetic spectrum, CD data can be obtained beyond the far- and near-UV. In some cases, chromophores show a CD signal at even higher wavelengths in the near-infrared (IR).

The spectral range that is being looked at somewhat dictates the **principal application** of protein CD spectroscopy. Based on the fundamental assumption that typical spectral profiles in the far-UV correlate with the relative content of the most common secondary structure elements, focus has traditionally been on the far-UV to determine the fractions of α -helices and β -strands in proteins. However, absolute determination of secondary structure by CD is less reliable than commonly perceived.

Figure 1: Spectral ranges of protein CD spectroscopy and the information they provide.



Modern protein CD spectroscopy is most powerful for **comparisons of secondary and tertiary structure** (often referred to as higher order structure) and makes use of both far- and near-UV. Firstly, one macromolecule can be

compared with another: wild-type versus mutant; different variants, isoforms, homologs; or biotherapeutics from different lots or batches. Secondly, the same molecule can be compared in different environments to examine the

impact on structure and stability of changes in buffer, excipients, pH, ionic strength, ligands, stress conditions, or changes over time resulting from prolonged storage.

Case Study: Structural Characterization of NISTmAb

The characterization of biotherapeutics in general and monoclonal antibody (mAb) therapeutics, in particular, is a complex task involving many functional and biophysical techniques. Until recently, it has been challenging to put different mAb studies into perspective, as common standards and procedures to assess these analytical techniques were missing.

This is despite the fact that mAbs are recognized as one of the most prevalent classes of biotherapeutics—since the beginning of this decade, global annual sales revenues for mAb products have continued to total more than half of that accrued by all biopharmaceutical products together [5].

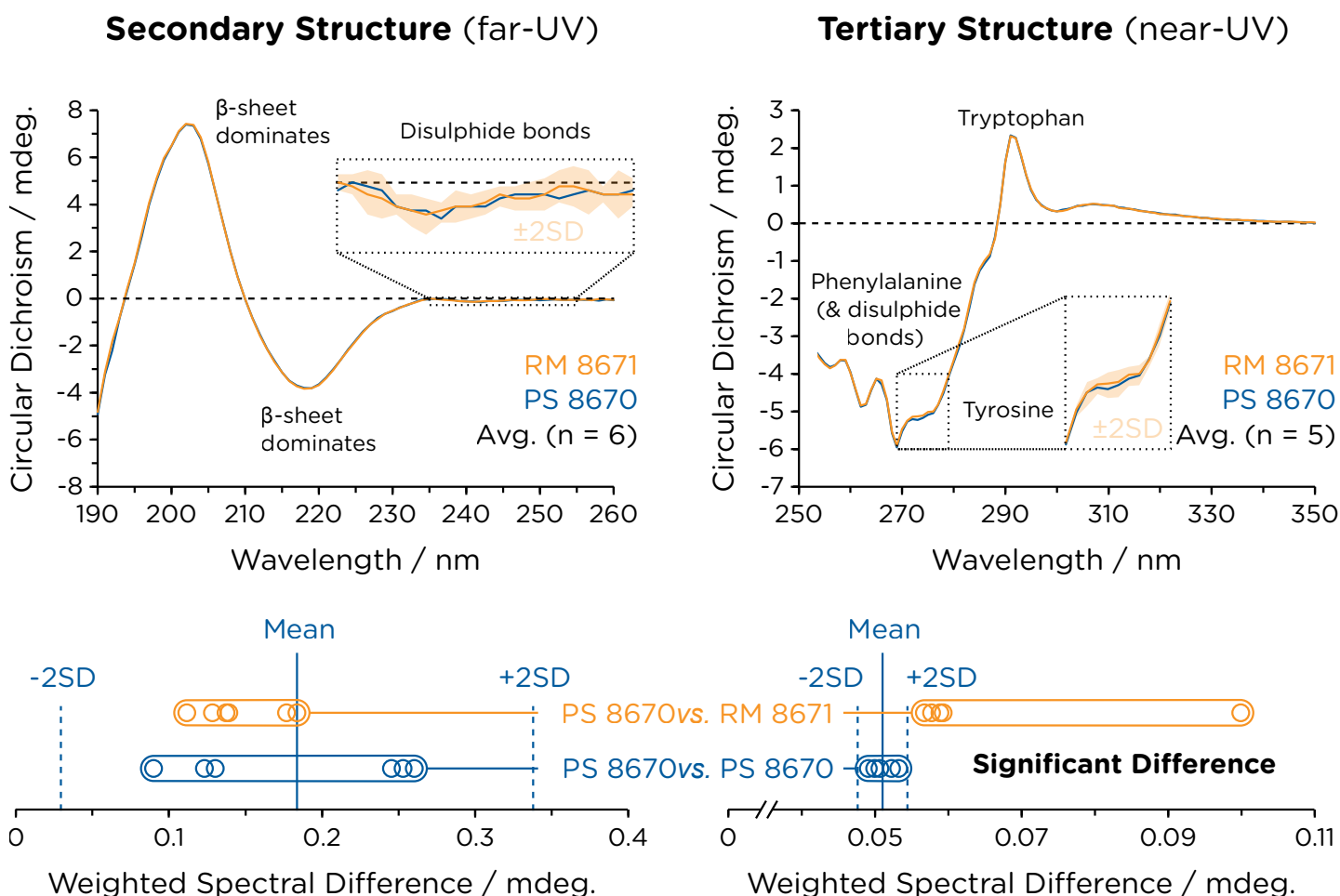
The solution to this problem was provided in the form of a comprehensively characterized and publicly avail-

able reference for the development of new mAb therapeutics: in 2016, the **National Institute of Standards and Technology (NIST)** in the USA undertook a holistic study using a humanized monoclonal antibody, the **NISTmAb** [6]. The study utilized the biophysical characterization techniques most commonly employed during biotherapeutic development with most recent results compiled in a mock Investigational New Drug (IND) filing

[7]. The NISTmAb is now available to biopharmaceutical companies as a representative test molecule to assist in method development and qualification and in evaluating and comparing instrument performance and analytical techniques. Applied Photophysics was approached by NIST to contribute to this project. The case study featured here is based on this collaboration.

A primary standard of the NISTmAb,

Figure 2: Characterization of secondary and tertiary structure of NISTmAb. Reference material RM 8671 was compared against primary standard PS 8670 and statistical significance of structural differences evaluated by means of Weighted Spectral Difference, applying an acceptance criterion of two standard deviations ($\pm 2SD$). For details of statistical analysis, see Section 4. Data was recorded with a Chirascan Q100.



Experimental:

Concentration: 1.28 mg/mL (far-UV), 0.8 mg/mL (near-UV)
Pathlength: 0.1 mm (far-UV), 10 mm (near-UV)
Repeat Scans: 5 per replicate

Temperature: 20°C
Step Size: 1 nm
Bandwidth: 1 nm
Time per Point: 1 s

PS 8670, was compared with the NISTmAb reference material, RM 8671, that had been derived from the primary standard by homogenization, aliquoting and dilution. The secondary and tertiary structure of PS 8670 and RM 8671 were characterized using a Chirascan™ Q100 automated CD spectrometer (Applied Photophysics). Samples were dialyzed into a common preparation of phosphate-buffered saline and diluted to obtain suitable concentrations for far- and near-UV measurements. Spectra were obtained for multiple independent replicates, corrected for the dialysate baseline and normalized by absorbance at 192 nm in the far-UV and 280 nm in the near-UV (Figure 2).

As expected for a monoclonal antibody, the far-UV spectrum is characteristic of a protein with a high β -sheet content, with a distinct peak at 202 nm and a negative peak at 218 nm. However, the far-UV spectra contain information beyond secondary structure elements—as highlighted in the inset plot, signals of lower amplitude around and above 230 nm arise from disulfide bonds and are expected to be sensitive to the dihedral angles of these bonds.

The profile of the near-UV spectra is much more complex as it is composed of overlapping contributions by the aromatic amino acid side chains of 24 tryptophan, 52 tyrosine, 50 phe-

nylalanine residues as well as 16 disulfide linkages. Although the near-UV spectra appear to be superimposable by visual inspection, statistical analysis reveals that the tertiary structure of RM 8671 is significantly different to that of PS 8670, while this is not the case for the secondary structure (lower panels in Figure 2). Such small spectral differences in the near-UV can only be found with state-of-the-art CD instruments that provide the required sensitivity. Moreover, the automation offered by a Chirascan Q100 enabled the reproducible generation of a sufficient number of replicates as required for robust statistical analysis.

3. Assessing Protein Stability Through Thermal Denaturation

The conformational stability of a biomolecule can be investigated by **equilibrium unfolding** experiments. Such experiments assume that the biomolecule can exist in folded and unfolded states and that a transition between these states is reversible. As the unfolded state hardly exists under normal conditions, conditions that favor unfolding are imposed on the biomolecule.

There are several ways to shift an equilibrium towards an unfolded state. A strategy commonly employed is the addition of a denaturant such as urea or guanidine hydrochloride. However, the simplest approach is to heat the sample i.e. perform a **thermal denaturation** experiment. Provided that the different conformational states generate different signal intensities at

identical wavelengths, unfolding can be followed spectroscopically. The mid-point transition temperature or **melting temperature**, T_m , at which the signal is halfway between the limits given by the two states, is characteristic for the stability of the biomolecule—the higher the T_m , the higher the thermal stability. Moreover, analysis of a thermal denaturation exper-

iment yields the **van't Hoff enthalpy**, ΔH_{vH} , which characterizes how sensitive the biomolecule is to thermal stress—the smaller the ΔH_{vH} the wider the transition. The approaches used for thermal denaturation experiments vary according to the information they provide and the time required (Box 2).

Box 2: Thermal denaturation analysis in theory

Conventionally, there are two different ways to perform thermal denaturation experiments.

In a **single-wavelength** temperature ramp, the temperature is increased continuously and the CD signal measured simultaneously at a chosen wavelength. This results in a sigmoidal curve, the inflection point of which corresponds to T_m .

In a **stepped-temperature** ramp, the temperature is increased stepwise, typically a few degrees Celsius at a time, and held constant at each step to allow for acquisition of a full spectrum. Such experiments yield more structural data, but determination of T_m is less precise as a lower number of temperatures are probed.

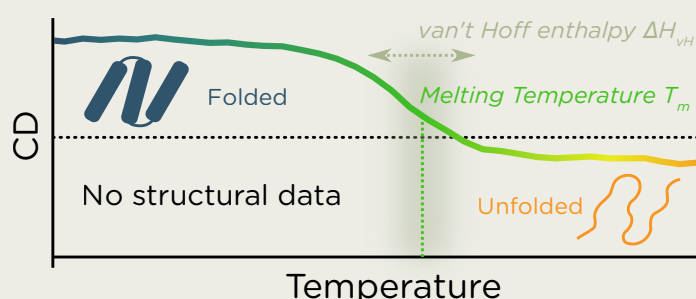
In contrast to these classical experiments, **continuous, multi-wavelength** thermal denaturation yields both comprehensive structural and thermodynamic information without an increase in experimental duration. Full spectra are acquired while the temperature is gradually increased. This implies that the temperature is not constant during the acquisition of each spectrum. However, this is accounted for by **global thermodynamic analysis**.

Plotting CD against temperature yields an unfolding curve for each wavelength. In a global thermodynamic analysis, each curve (two are highlighted in the figure) is fitted with a sigmoidal function of the form

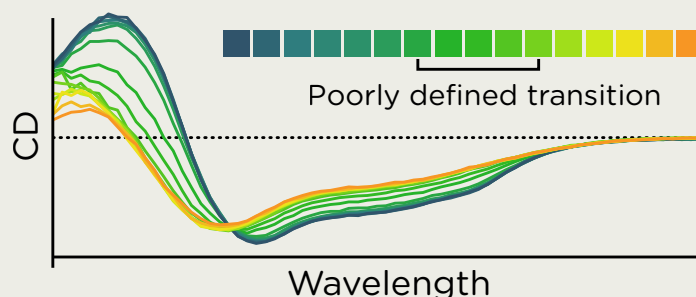
$$CD(T) = \frac{(m_F T + b_F) - (m_U T + b_U)}{1 + e^{\frac{\Delta H_{vH}}{R} \left(\frac{1}{T_m} - \frac{1}{T} \right)}} + m_U T + b_U$$

as derived from the Gibbs-Helmholtz equation [8]. This function contains both local and global fitting variables. The thermodynamic characteristics, the melting temperature T_m and the van't Hoff enthalpy ΔH_{vH} , are **global variables**, i.e. each fit is calculated with the same values for these variables to describe the same position and width of the transition for all fits. The inflection point of the fit corresponds to T_m . Combining unfolding curves for a large number of wavelengths enables precise determination of T_m and distinction between minor differences of thermal stability in protein comparisons.

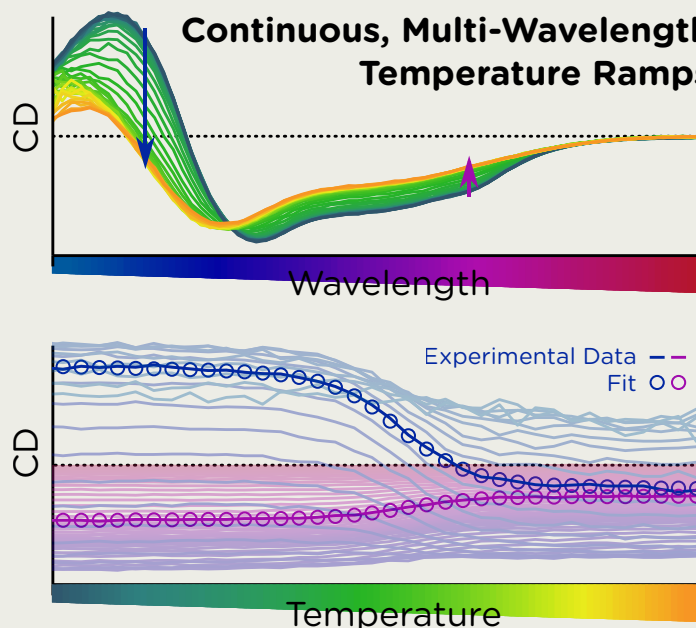
Single-Wavelength Temperature Ramps



Stepped-Temperature Ramps

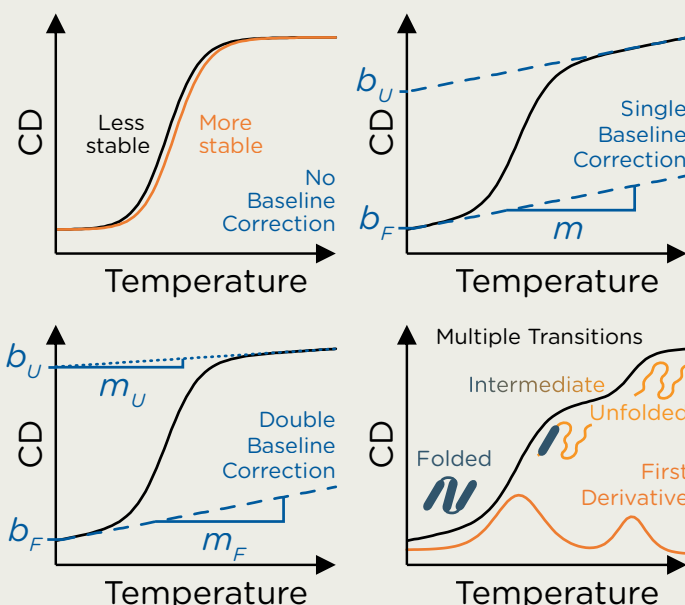


Continuous, Multi-Wavelength Temperature Ramps



In addition, every fit has **local variables** that describe the linear regions before and after the transition. These pre- and post-transition regions may show a constant signal. In this case, each fit is described by local variables b_F and b_U , i.e. the CD signals corresponding to the completely folded and unfolded conformation at a certain wavelength, respectively. However, there may be a signal change that does not result from a structural change. In these cases, a **baseline correction** is required. The baselines for pre- and post-transition regions are described by linear functions and can either have the same slope (single-baseline correction), or different slopes (double-baseline correction).

If there are **multiple transitions**, due to additional conformational states of unfolding, the fitting function becomes more complex and the number of variables increases accordingly e.g. four global variables for two transitions. The number of transitions must be known to choose the correct fitting function but identifying multiple transitions can be difficult if they are close together. If there is uncertainty, calculating the numerical first derivative of the unfolding curve can facilitate discrimination between transitions as peaks in the derivative correspond to inflection points in the unfolding curve and, thus, reveal multiple transitions.



Case Study: Stability of α -Chymotrypsin

As an illustration of the wealth of data on protein structure and stability that can be obtained from a thermal denaturation experiment, α -chymotrypsin, a proteolytic enzyme with a structure dominated by anti-parallel β -strands arranged in β -barrels rather than β -sheets, was heated in 15 mM citrate-phosphate buffer of pH 7 (Figure 3).

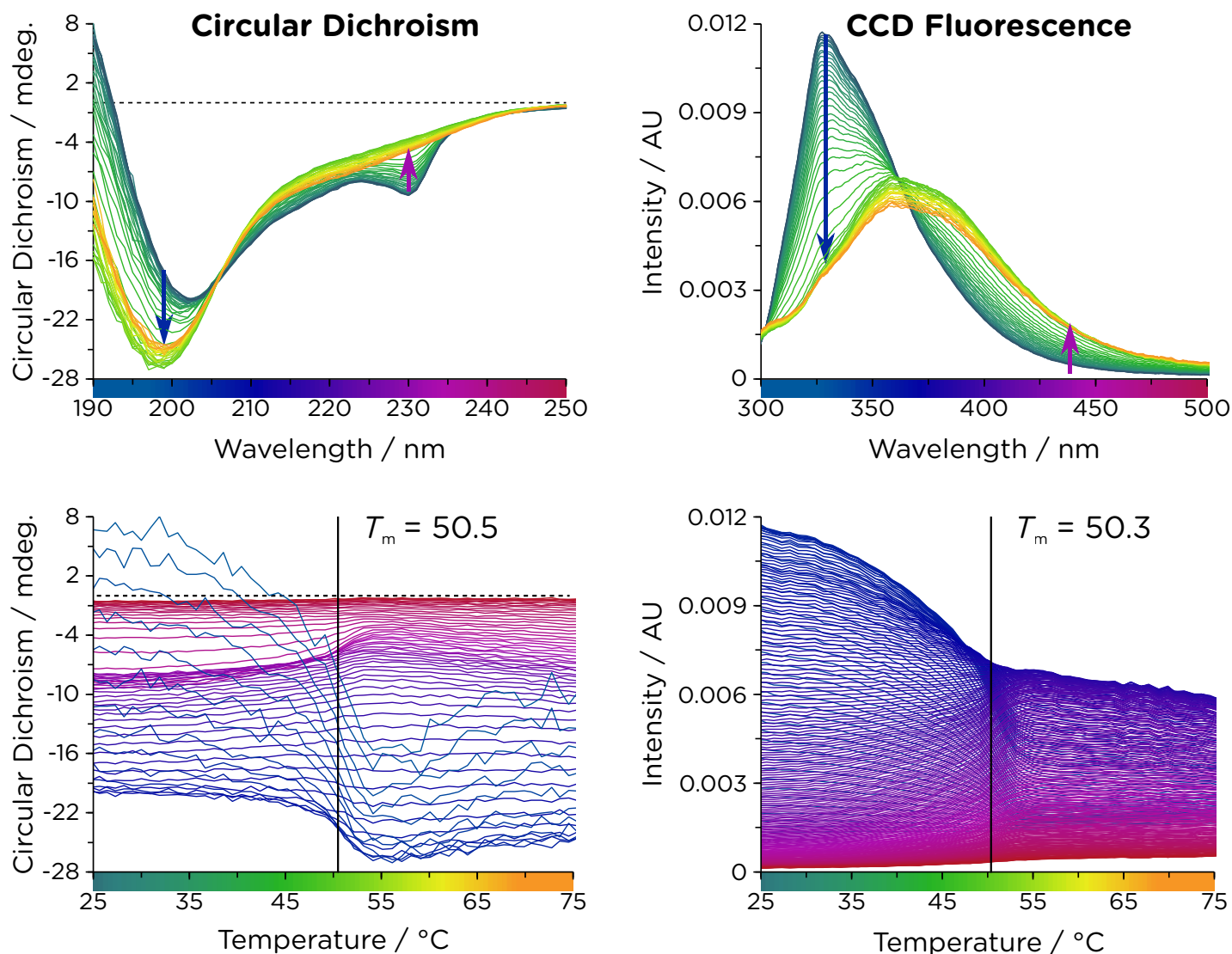
Using a Chirascan V100 CD spectrometer (Applied Photophysics), the experiment was performed as a continuous, multi-wavelength temperature ramp, recording the actual sample temperature with an in-sample temperature probe while heating from 25°C to 75°C at a rate of 0.5°C/min. The entire experiment was completed in approximately 100 minutes. This duration was similar to classical thermal denaturation experiments even though **three different signals** were acquired **in the same experiment**: far-UV CD, absorbance (monitored simultaneously, data not shown) and a fluorescence emission spectrum were recorded after each CD spectrum. In total, 56 CD and fluorescence spectra were recorded. A Chirascan **CCD Fluorometer** (Applied Photophysics) recorded each full fluorescence emission spectrum within seconds.

The far-UV CD spectra of α -chymotrypsin before unfolding have a profile that is different compared to other proteins that mainly contain β -strands. The negative peak that is located at about 220 nm for typical β -sheet proteins is shifted to about 200 nm. This is assumed to be caused by the distorted structure of the protein's β -barrels [9]. Moreover, there is an additional negative peak at 230 nm which is not found in typical β -sheet spectra. Upon thermal denaturation, the former peak shifts to even lower wavelengths suggesting increased distortion and the latter disappears.

The data was analyzed using Thermodynamic Analysis software (Applied Photophysics) to obtain thermodynamic characteristics. Making use of the entire CD data for a global fit, a melting temperature of $T_m = 50.5^\circ\text{C}$ was obtained.

As α -chymotrypsin contains 18 aromatic amino acids, fluorescence emission of these fluorophores could be followed during the temperature ramp. The emission spectra show both a decrease in maximum intensity and a shift of the maximum to higher wavelengths with increasing temperature. Whereas the former results from collisional quenching as diffusion increases with temperature, the latter indicates that some buried aromatic amino acids are relocated upon unfolding of the protein. As these residues become more exposed to the buffer, they partake in a solvent relaxation process: upon excitation, the charge distribution of the fluorophore changes so that the polar water molecules reorient around it. Thereby, they lower the energy of the excited state and, thus, the wavelength of the emission maximum increases [10].

Figure 3: Continuous, multi-wavelength thermal denaturation of α -chymotrypsin. Structural and thermodynamic information was obtained, recording far-UV CD and fluorescence emission spectra in a single experiment. Fluorescence emission spectra are normalized to account for temperature dependent quenching and corrected for dark current offset. Data was recorded with a Chirascan V100.



Experimental:

Concentration: 0.1 mg/mL
Pathlength: 2 mm
Heating Rate: 0.5°C/min

Circular Dichroism:

Step Size: 1 nm
Bandwidth: 1 nm
Time per Point: 1 s

CCD Fluorescence:

Excitation Wavelength: 285 nm
Excitation Bandwidth: 8 nm
Boxcar Width: 1 nm
Integration Time: 1 s
Extra Delay: 0 ms
Scans to Average: 6

The fluorescence data was used to corroborate the melting temperature obtained from the CD data. However, while the CD signal at a given wavelength is practically independent of temperature, fluorescence emission intensity generally decreases with increasing temperature. Therefore, to account for this effect, the raw emission spectra were automatically normalized by area by the Thermodynamic Analysis software.

Fluorescence spectra shown in Figure 3 are those obtained after this processing. By subjecting the processed fluorescence data to the same analysis as the CD data, a similar melting temperature of $T_m = 50.3^\circ\text{C}$ was obtained. This suggests that secondary and tertiary structure of α -chymotrypsin as assessed by far-UV CD and fluorescence, respectively, show a similar response with regards to thermal stability.

In summary, this case study demonstrates how the thermal stability of proteins can be confidently characterized by monitoring both CD and fluorescence signals in a **continuous, multi-wavelength** experiment to obtain comprehensive information about both structure and thermodynamic properties.

4. Evaluating Statistical Significance of Changes Detected in Higher Order Structure

Thorough and reliable protein characterization methods are of critical importance, particularly in the biopharmaceutical industry where the most minor structural change could affect the **safety, quality, efficacy or manufacture of a biotherapeutic**. This is reflected in the ever-increasing demands by regulatory authorities such as the FDA and EMA for objective, statistically-validated data.

Although acknowledging such requirements, developers of biotherapeutics are challenged whenever methodological limitations or sample availability prevent them from collecting such data. In fact, the FDA retracted its draft guidance on **statistical approaches to evaluate analytical similarity**, nine months after its release (September 2017) following concerns by the industry about the high number of reference product lots to be sourced and the lot-to-lot variability of reference products.

While reference availability will remain a matter of concern, technical limitations can be overcome. This holds true particularly for **higher order structure (HOS) comparisons** by CD spectroscopy. This type of analysis infers information about changes in HOS from pairwise comparisons of spectra obtained under different conditions. Changes in HOS must be detected and followed throughout biotherapeutics development, for example, to confirm that a drug is not affected by a minor change of the formulation buffer or to demonstrate the similarity of multiple production lots. In biosimilar development, identification of structural differ-

ences between **biosimilar** and originator at early stages minimizes residual uncertainties that would need to be resolved in downstream processes. Therefore, finding differences early on is as crucial as confirming the similarity between biosimilar and originator at later stages where such evidence can strengthen the **totality of evidence for regulatory submission**.

Although CD spectroscopy is outstanding in its capability of providing information about both secondary and tertiary structure, its usefulness for HOS comparisons has been undervalued in the past because comparisons were based on subjective, visual evaluation of CD spectra. HOS comparisons were given low relevance not because such data was considered uninformative, but because conventional CD spectroscopy failed to meet the requirements for a quantitative analysis. With the ability of modern CD spectrometers such as the Chirascan Q100 to enable objective, statistically-validatable HOS comparisons, CD spectroscopy is now recognized as a crucial part of the biophysical characterization process where HOS comparisons are essential for defining **critical**

quality attributes of biotherapeutics.

The **high sensitivity** of CD instruments that make use of solid-state detectors now enables detection of even minor changes, not only in secondary structure in the far-UV, but also in tertiary structure in the near-UV where a CD signal is typically lower by orders of magnitude.

More importantly, the use of flow cells in combination with automated liquid handling now eliminates errors associated with manual handling of samples and cuvettes. Besides increased **reproducibility**, CD analyses can be performed in a timely manner with the precision and the number of replicates required for robust statistical analysis. The risk of user-bias associated with visual comparisons is removed and the statistical significance of spectral differences confirmed objectively. These innovative developments are elevating CD spectroscopy from Tier 3 (raw data/graphical comparison) to Tier 2 (quality range method) for HOS comparison as referred to in the tiered approach developed by the Office of Biostatistics and Office of Biotechnology Products, CDER/FDA.

Case study: Forced Degradation of a Monoclonal Antibody

To demonstrate the detection and statistical analysis of minor changes in HOS, a monoclonal antibody, IgG1, was subjected to different stress conditions in a forced degradation study. Different sample pre-treatments were expected to induce oxidation, asparagine (Asn) deamidation / aspartate (Asp) isomerization or glycation of the antibody. Stress conditions were stopped by dialysis against a common buffer (phosphate buffered saline pH 7.4).

For every stress condition, CD spectra for five **independent replicates** were measured. For each replicate, three repeat scans were acquired, averaged and buffer-corrected.

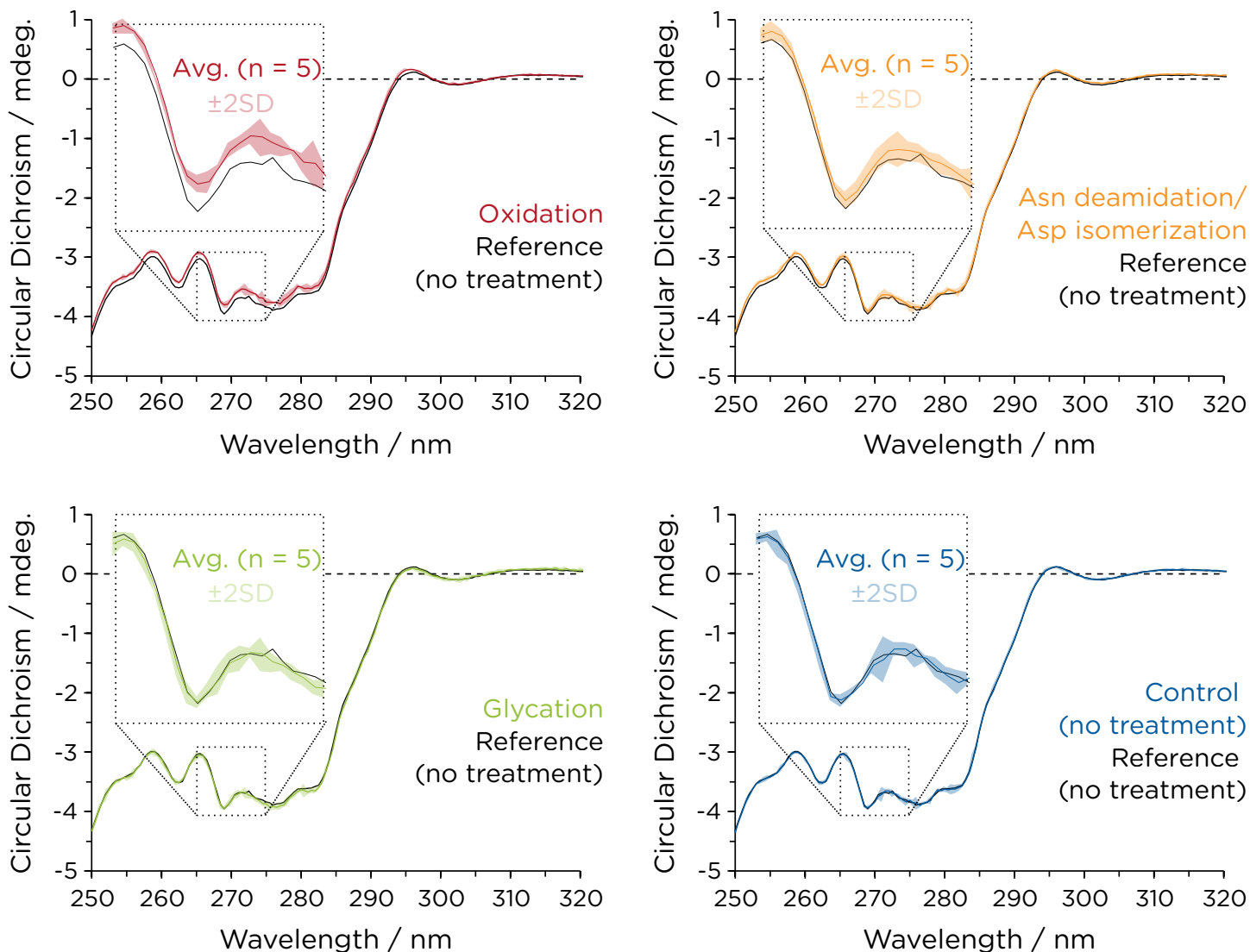
Moreover, simultaneous acquisition of absorbance together with the CD allowed for **normalization** (by absorbance at 280 nm). This is an important step in data analysis, as it excludes any apparent differences between replicate spectra that actually result from slight differences in concentration rather than from structural differences.

The near-UV spectra of all samples have a similar **fingerprint profile** with contributions from aromatic amino acids and disulfide bonds (Figure 4). While a difference between the oxidation spectrum and the reference spectrum is fairly obvious from visual inspection, it is less clear for the other stress conditions. In particular, the glycation spectrum looks as similar to the reference as the control spectrum does to the reference. However, minor alterations in tertiary structure can result, for example, from changes in

the dihedral angles of disulfide bonds that are so subtle that they elude visual inspection.

Statistical analysis is required for an objective, **unbiased data evaluation**. The current preference within the pharmaceutical industry is towards using the **Weighted Spectral Difference (WSD)** method [11] for a comparative analysis to assess the similarity of two spectra. Highly transparent, this analysis is increasingly accepted by biopharmaceutical companies and regulatory authorities.

Figure 4: HOS comparison: forced degradation of IgG1 samples assessed by near-UV CD. The monoclonal antibody was subjected to the stress conditions as indicated in Figure 5; near-UV spectra shown are normalized by absorbance at 280 nm. Data was recorded with a Chirascan Q100.



Experimental:

Concentration: 1.08 mg/mL (far-UV), 6.48 mg/mL (near-UV)
 Pathlength: 0.1 mm (far-UV), 5 mm (near-UV)
 Repeat Scans: 3 per replicate

Temperature: 20°C
 Step Size: 1 nm (far-UV), 0.5 nm (near-UV)
 Bandwidth: 1 nm (far-UV), 1.5 nm (near-UV)
 Time per Point: 1 s

Figure 5: Statistical analysis of results from Figure 4 by means of Weighted Spectral Difference. All stress conditions resulted in statistically significant changes in IgG1 tertiary structure as assessed by near-UV CD.

Sample pretreatment

0.3% H₂O₂, 20°C, 3 hours

pH 8.5, 40°C, 1 week

2 M glucose, 40°C, 1 week

Dialysis only

No treatment

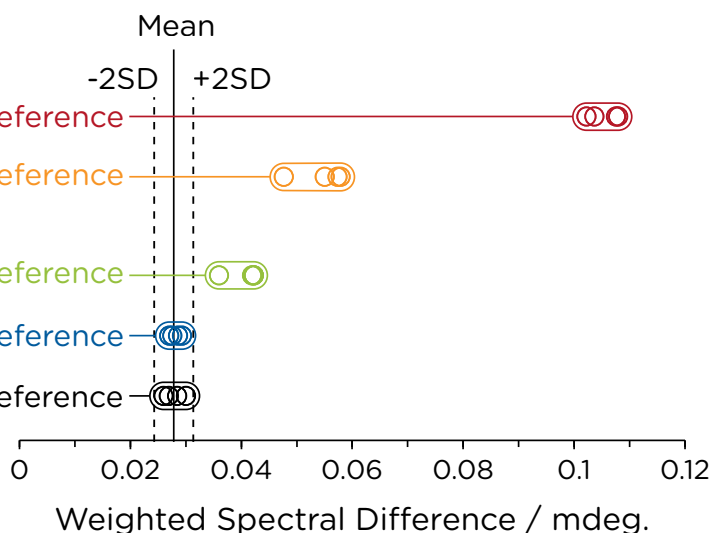
Oxidation vs. Reference

Asn deamidation/
Asp isomerization vs. Reference

Glycation vs. Reference

Control vs. Reference

Reference vs. Reference



In brief, a difference spectrum is calculated from the two spectra that are to be compared and then a wavelength-dependent weighting is applied based on the reference spectrum (Box 4). This weighting reduces the relative contribution of low-signal regions where spectral variation stems mainly from noise. Ultimately, the spectral results are converted into a numerical value, WSD, as a measure for similarity. The smaller the WSD, the greater the similarity of the compared spectra.

For statistical analysis, WSD values are first calculated for comparisons of reference replicates among each other to assess the variability of the reference spectra. In the example (Figure 4), the resulting five WSD values (one

for each reference replicate compared to the remaining reference replicates) are shown in black together with the mean of these WSD values and a range defined by twice the standard deviation. This range was chosen as an acceptance criterion which allows the data to be subjected to a **quality range test** as recommended by the FDA for Tier 2 critical quality attributes.

To this end, WSD values were calculated for comparisons between individual sample replicates and the reference. As can be seen in Figure 4, all WSD values for the control fall within the acceptance range, whereas those for the different stress conditions do not. This shows that even the glycation conditions, which resulted in **spectra**

highly similar to the reference and virtually indistinguishable from the control, lead to a **statistically significant change** in tertiary structure. Moreover, the plot of WSD values shows that the detected, significant differences resulting from the different stress conditions are of different magnitude.

In summary, minor differences between CD spectra were detected and found to be statistically significant, reflecting changes in tertiary structure of a monoclonal antibody after subjection to various stress conditions. This forced degradation study thus illustrates how minor differences, that most likely would be overlooked by visual inspection, can be revealed by statistical analysis.

Box 3: Weighted Spectral Difference

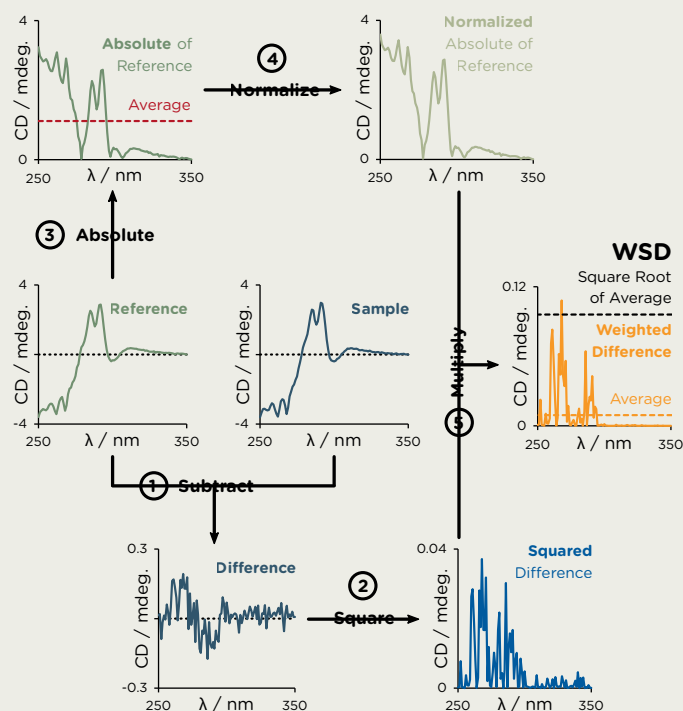
Comparison of two spectra by the Weighted Spectral Difference method yields a single value, a WSD, as a measure for their similarity according to the following equation:

$$WSD = \sqrt{\sum_{i=1}^n \left[\left(\frac{1}{n} \right) \left(\frac{|y_{Ai}|}{|y_A|_{ave.}} \right) (y_{Ai} - y_{Bi})^2 \right]}$$

To obtain the WSD for the comparison of a reference spectrum (y_{Ai}) with a sample spectrum (y_{Bi}), first the sample spectrum is subtracted from the reference spectrum (1). The resulting **difference spectrum** (blue) is then squared so that negative values cannot cancel out positive values (2).

A **weighting** based on the reference (gray) is then applied to this squared difference: first, the absolute values of the reference are taken, again to account for negative signals (3). The absolute reference is then normalized (4) by dividing through its average (red) and multiplied by the squared difference spectrum (5) to obtain a weighted difference spectrum (orange, solid line).

Finally, the WSD is obtained by calculating the average intensity of the weighted difference spectrum (orange, dashed line), by summing over all datapoints (i) and dividing by their total number (n), and taking its square root.



5. The Physical Principles Behind Circular Dichroism

Similar to UV/vis spectroscopy, CD spectroscopy is an absorbance technique in which a light source generates a beam which undergoes wavelength selection and then passes through a sample and reaches a detector. The difference between the two techniques lies in the polarization of the generated light (Box 5): UV/Vis spectroscopy uses unpolarized light, while CD spectroscopy uses **circularly polarized (CP) light** that is modulated between left and right circular polarizations.

A CD spectrometer records a **differential absorbance** as a function of wavelength, i.e. CD is the difference in absorbance between left-handed circularly polarized (L-CP) and right-handed circularly polarized (R-CP) light:

$$CD = \Delta A(\lambda) = A(\lambda)_{L-CP} - A(\lambda)_{R-CP}$$

Correspondingly, CD spectra can assume both positive and negative values: the signal at a certain wavelength is positive when the L-CP light is absorbed more than the R-CP light, and negative when the R-CP light is absorbed more than the L-CP light (Figure 6).

The recorded difference in absorbance is extremely small—several orders of magnitude smaller than the

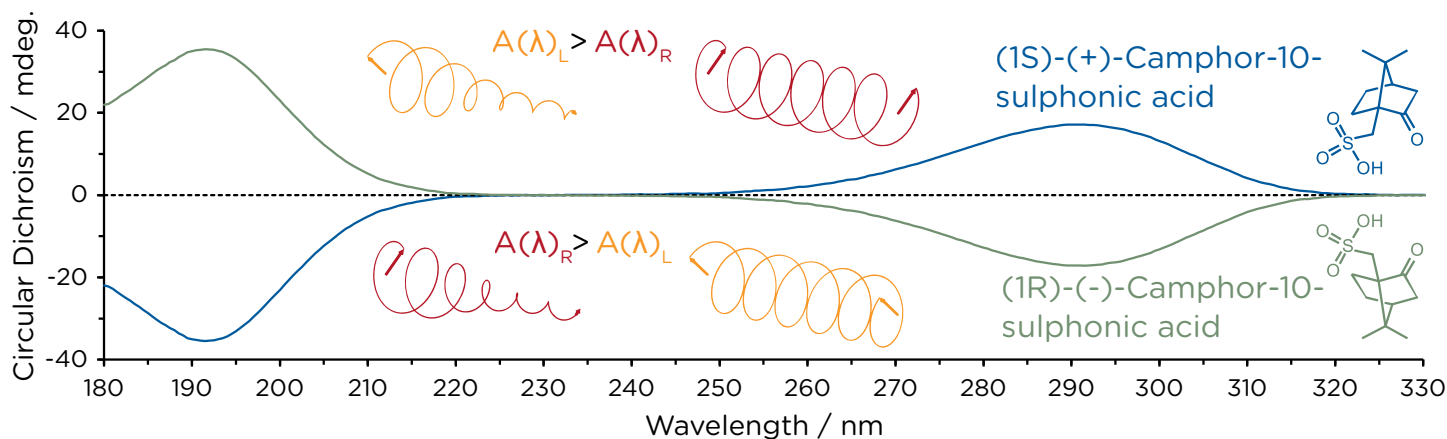
total absorbance of a typical sample—thus CD spectrometers must have high sensitivity. One key technical advancement that has significantly increased the sensitivity of CD spectrometers has been the introduction of **avalanche photodiode detectors**, replacing conventional photomultiplier detectors to reduce background noise and thus facilitate the detection of minor changes even in the near-UV range where the magnitude of CD signals is typically low.

To generate a CD signal, a molecule must fulfil two requirements: it must possess a **chromophore** (absorb light) and exhibit **chirality** (not be superimposable on its mirror image). Two

isomers that are non-superimposable mirror-images of a chiral molecule are called enantiomers. Physical and chemical properties of a pair of enantiomers are identical with two exceptions: the way in which they interact with polarized light and the way in which they interact with other chiral molecules.

Figure 6 shows an example of a chiral absorbing molecule: camphor sulfonic acid (CSA) exists as two enantiomers. The CD spectrum of (1S)-(+)-CSA exhibits a positive peak at 290.5 nm and a negative peak at 191 nm. The CD spectrum of the other enantiomer, (1R)-(-)-CSA, has exactly the same profile, but is mirrored at the x-axis.

Figure 6: CD spectra of Camphor sulfonic acid (CSA). CSA is a chiral molecule and exists as two enantiomers which are non-superimposable mirror-images of each other. Their corresponding CD spectra are mirrored at the x-axis. Positive CD signals are obtained at wavelengths where the left-handed component of circularly polarized light is absorbed more strongly than the right-handed component and negative when it is the other way around.

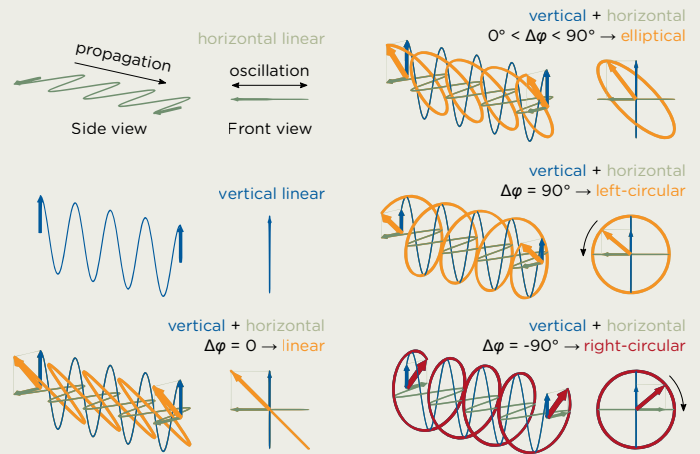


Box 4: Polarization Basics

Light is an **electromagnetic wave**, and polarization describes the orientation of its electric or its magnetic vector. For example, sun light that is reflected at a certain angle from the sea surface is **linearly polarized**: the electric vector oscillates along a single line and so the wave propagates through space within a plane. This plane can be rotated at any angle around the direction in which the wave propagates and so have different orientations, for example horizontal or vertical.

Any polarized state of light can be described as the resultant of two linearly polarized states at right angles to each other. For instance, combining a horizontal- with a vertical-linearly polarized wave of equal amplitude and in phase with each other results in a light wave that is linearly polarized and at 45° to the planes of the two combined waves.

If the two polarization states are out of phase, the resultant wave is **elliptically polarized**. A special case occurs if the phase difference $\Delta\phi$ of the vertical component relative to the horizontal component is a quarter of the wavelength: this results in **circularly polarized** (CP) light, where the electric vector rotates and, thus, describes a helix while propagating through space. This helix can



be either right-handed (R-CP light), i.e. if $\Delta\phi$ is negative (-90°), the rotation is clockwise when viewed towards the light source, or left-handed (L-CP light), i.e. if $\Delta\phi$ is positive (90°), the oscillation is counterclockwise. These two polarization states are non-superimposable mirror images, as are the threads of the right and left pedals of a bicycle.

References

- [1] Y. Liu et al. 2017, "Ratiometric fluorescence sensor for the microRNA determination by catalyzed hairpin assembly", *ACS Sensors*, 2, 1430-1434.
- [2] A. Varizhuk et al. 2017, "The expanding repertoire of G4 DNA structures", *Biochimie*, 135, 54-62.
- [3] H. Yang et al. 2017, "A novel chimeric lysin with robust antibacterial activity against planktonic and biofilm methicillin-resistant *Staphylococcus aureus*", *Scientific Reports*, 7, 40182.
- [4] R. Selegård et al. 2017, "Folding driven self-assembly of a stimuli-responsive peptide-hyaluronan hybrid hydrogel", *Scientific Reports*, 7, 7013.
- [5] D. M. Ecker et al. 2015, "The therapeutic monoclonal antibody market", *mAbs*, 7, 9-14.
- [6] NIST, "NIST Monoclonal Antibody Reference Material 8671", 2018. [Online]. Available: <https://www.nist.gov/programs-projects/nist-monoclonal-antibody-reference-material-8671>. [Accessed: 12-Oct-2018].
- [7] J. Schiel and C. Vessely, "NISTmAb common technical document case study", presented in workshop at the 6th International Symposium on Higher Order Structure of Protein Therapeutics (HOS 2017). [Online]. Available: <https://www.casss.org/page/HOS1700>. [Accessed: 12-Oct-2018].
- [8] N. J. Greenfield 2007, "Using circular dichroism collected as a function of temperature to determine the thermodynamics of protein unfolding and binding interactions", *Nature Protocols*, 1, 2527-2535.
- [9] P. Manavalan and W. C. Johnson 1983, "Sensitivity of circular dichroism to protein tertiary structure class" *Nature*, 305, 831-832.
- [10] J. R. Lakowicz 2006, "Principles of Fluorescence Spectroscopy", 3rd Edition, Boston, MA: Springer US.
- [11] N. N. Dinh et al. 2014, "Quantitative spectral comparison by weighted spectral difference for protein higher order structure confirmation" *Analytical Biochemistry*, 464, 60-62.